Robotica (1998) volume 16, pp. 219–225. Printed in the United Kingdom © 1998 Cambridge University Press

Accurate modelling of compliant grippers using a new method

M.H. Refaat and S.A. Meguid

Engineering Mechanics and Design Labotatory, Department of Mechanical and Industrial Engineering, University of Toronto, 5 King's College Road, Toronto, ON M5S 3G8 (Canada)

(Received in Final Form: April 26, 1997)

SUMMARY

Current techniques which have been devised for motion planning and control of compliant multi-fingered grippers are based on the assumption of a constant compliance. The present investigation was undertaken to examine the validity of this assumption. To this end, the variational inequalities approach and the finite element method were used to formulate the general frictional contact problem. A two-step algorithm, which employs Quadratic Programming and non-differential optimization algorithms, is used to solve the resulting variational inequality and to provide the contact characteristics of compliant grippers.

The proposed method is applied to a case study involving a multi-fingered compliant gripper. The equivalent stress contours and the compliance of the system were obtained and analyzed. The proposed approach, which can be applied to any contact problem in robotics, overcomes most of the difficulties and approximations evident in current simplified contact analysis techniques.

KEYWORDS: Compliant grippers; Accurate modelling; Quadrating programming; Robotics.

1. INTRODUCTION

Contact conditions, compliance, and friction play major roles in the grasping, manipulation and assembly of objects. This is particularly evident in cases where compliant multi-fingered grippers are used to accurately and repeatedly assemble delicate soft objects at low velocities (Figure 1).

In spite of the fact that the actual distribution of the forces acting on the grasped object and therefore the effective compliance of the gripper change with the applied grasping force, almost all papers surveyed by the authors to date indicate that the assumption of point contact compliance is used in all dynamic modelling and control analyses. For a detailed review of the literature on the subject see the work of Cutkosky,[1,2] Cutkosky and Kao,[3] Rosheim,[4] Venkataraman[5] and Speeter.[6]

Numerous analytical approaches have been proposed to treat contact problems as in Johnson[7] and Gladwell.[8] However, in view of the complexity of the resulting equations, contact problems are treated using numerical techniques, with the finite element method being the most appealing; see, e.g. Kikuchi and Oden.[9]

A common FE approach in the treatment of this class of problems is to develop contact elements which are used to imposed the kinematic contact conditions of the problem. Naturally, these elements are assembled in the global stiffness matrix of the bodies in contact. However, this traditional approach suffers from major difficulties, see Böhm.[10] The first is concerned with the introduction of user defined penalty parameters for the normal compliance between the two bodies so as to avoid interpenetration. The selection of these parameters affect the convergence and accuracy of the resulting solution. The second is related to the non-differentiability of the most commonly used friction law that of Coulomb. The third is concerned with the increased size of the problem and the disturbance to the banded sparse global stiffness matrix commonly observed in finite element formulations.

To overcome these difficulties, the current problem is treated using a more rigorous and consistent approach, known as the variational inequalities (VI) approach. The variational inequalities formulation removed most of the mathematical inconsistencies present in the traditional variational finite element methods. In addition, Starvroulakis et al.[11] have shown that computational economy is achieved by eliminating the special contact elements. Accordingly, two aspects of the work are examined. The first is concerned with the determination of the true compliance of a multi-fingered compliant gripper and the second with the resulting von Mises stress contours. This paper is divided into 5 sections. Following this brief introduction, section 2 outlines the mathematical formulations and the newly developed variational inequality. In section 3, we describe the adopted solution technique, while in section 4 we provide a case study involving a compliant gripper. Finally, we concoude the paper in section 5.

2. MATHEMATICAL FORMULATIONS

An important aspect of all classes of contact problems is the imposition of the kinematic and stress constraints. The contact constraints are governed by: (i) the magnitude of the normal contact stress; being less than or equal to zero and; (ii) the displacement of the contacting surfaces must avoid penetration. These two conditions can be given mathematically according to the following:

$$\mathbf{N}\cdot\mathbf{u}-g\le 0,\quad \sigma_n\le 0,\quad \sigma_n(\mathbf{N}\cdot\mathbf{u}-g)=0\quad \text{on } \Gamma_c \qquad (1)$$

https://doi.org/10.1017/S026357479800054X Published online by Cambridge University Press

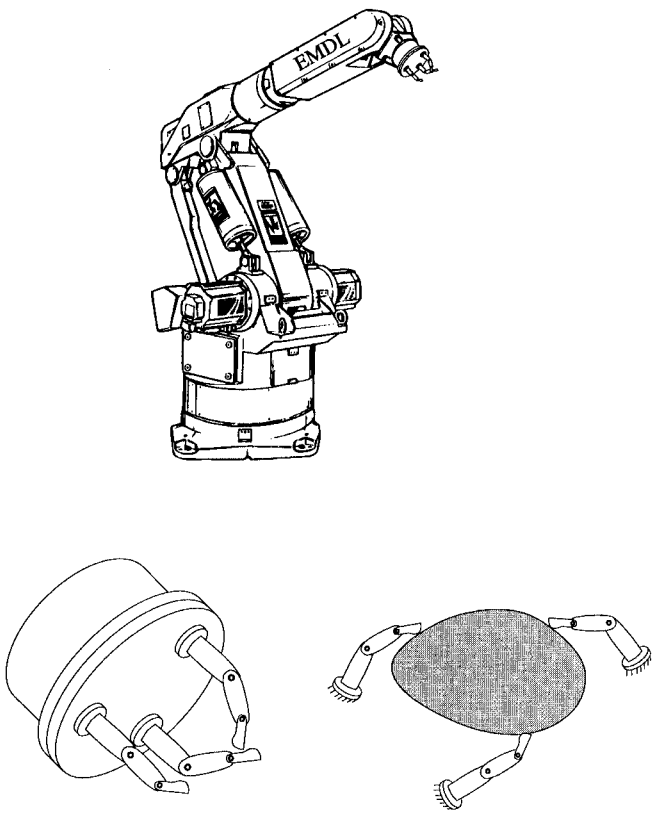


Fig. 1. Robotic dextrous grippers.

with the gap g given by

$$g = N_3(\psi - \phi) \tag{2}$$

See Figure 2 for details.

In contact problems, restrictions imposed upon admissible displacement and stress fields are not equalities but rather inequalities. Accordingly, the variational inequalities approach can be viewed as being the formulation of the principle of virtual work in inequality form. Refaat and Meguid.[12,13] have shown that adopting the variational inequalities approach, the current contact problem (Figure 3) can be stated as finding the displacement vector $\mathbf{u}$ everywhere in Ω such that

$$B(\mathbf{u}, \mathbf{w} - \mathbf{u}) + J(\mathbf{u}, \mathbf{w}) - J(\mathbf{u}, \mathbf{u}) \geq f(\mathbf{w} - \mathbf{u}) \tag{3}$$

for all $\mathbf{w}$ subject to the following boundary and kinematic contact conditions:

$$\mathbf{u} = \mathbf{w} = \mathbf{0} \quad \text{on } \Gamma_d \quad \text{and} \quad \mathbf{N} \cdot \mathbf{u} - g \leq 0 \quad \text{on } \Gamma_c \tag{4}$$

In expression (3), the different terms are defined as follows:

$$B(\mathbf{u}, \mathbf{v}) = \int_{\Omega} \sigma(\mathbf{u})_{ij} \epsilon_{ij}(\mathbf{v})\, dx\, dy\, dz, \tag{5}$$

$$J(\mathbf{u}, \mathbf{v}) = \int_{\Gamma_c} -\mu \sigma_n(\mathbf{u})\, |v_t|\, ds, \tag{6}$$

and

$$f(\mathbf{v}) = \int_{\Omega} f_i v_i\, dx\, dy\, dx + \int_{\Gamma_t} t_i v_i\, ds. \tag{7}$$

The physical meaning of variational inequality (3) can be explained as follows. The term $B(\mathbf{u}, \mathbf{w} - \mathbf{u})$ represents the virtual work of the elastic resistance of deformation from the configuration $\mathbf{u}$ to that of $\mathbf{w}$, while the two terms $J(\mathbf{u}, \mathbf{w})$ and $J(\mathbf{u}, \mathbf{u})$ together represent the virtual work dissipated in friction on the contact surface Γ_c and the term $f(\mathbf{w} - \mathbf{u})$ represents the virtual work of the external forces. Therefore, variational inequality (3) can be interpreted as follows: for any virtual displacement from the configuration $\mathbf{u}$, that satisfies the kinematic contact condition, the virtual work done by the external forces is not adequate to overcome the elastic resistance and the friction on the boundary Γ_c. Hence, $\mathbf{u}$ is the equilibrium configuration for all feasible virtual displacements.

The advantage of using the VI approach in solving contact problems is that it enables the use of traditional structural finite elements without the need for special contact elements to impose the necessary kinematic contact conditions, see Refaat and Meguid.[12] Instead, the

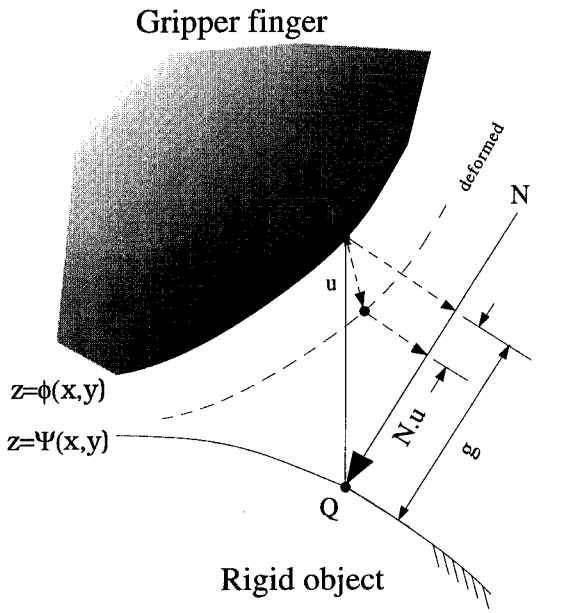


Fig. 2. The kinematic contact condition.

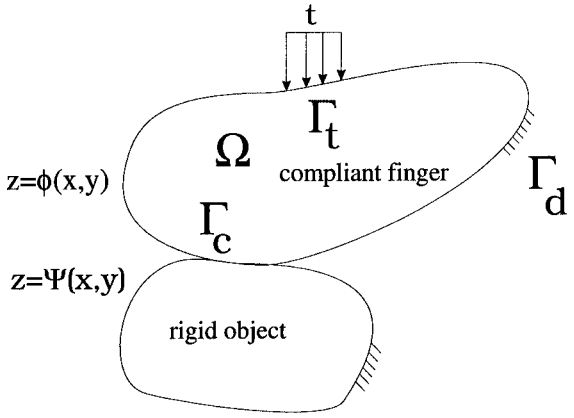


Fig. 3. Contact between a gripping finger and an object.

https://doi.org/10.1017/S026357479800054X Published online by Cambridge University Press

kinematic contact conditions are imposed *explicitly* in the solution algorithm.

3. SOLUTION TECHNIQUE

The main difficulty with the current problem is that there is no direct solution technique for VI(3) available at the moment with all its terms included. A two step algorithm, which makes use of two special reduced problems (Figure 4), will be adopted. The following two sub-sections describe the Quadratic programming approach used in the first step and the development of a new successive approximation method for the second step.

3.1 Special Case I: prescribed tangential stresses on Γ_c

If the tangential stresses σ_t are known along the boundary Γ_c, then variational inequality (3) reduces to:

$$B(\mathbf{u}, \mathbf{w}-\mathbf{u}) \geq f_1(\mathbf{w}-\mathbf{u}) \tag{8}$$

where

$$f_1(\mathbf{v}) = f(\mathbf{v}) + \int_{\Gamma_c} \sigma_t v_t \, ds \tag{9}$$

and $f(\mathbf{v})$ is as defined in (7).

Earlier solutions of variational inequality (8) were of the penalty type, see e.g. Kikuchi and Oden.[9] They suffered from the disadvantages of being slow to converge and their accuracy depends upon a user defined penalty parameter, see Böhm[10] and Meguid et al.[14] To overcome these difficulties, the technique of quadratic programming is adopted in the current work. The use of quadratic programming in the treatment of special case I is based on the fact that the solution of variational inequality (8) is equivalent to solving the following minimization problem (see Glowinski et al.[15]):

$$\min \left(\tfrac{1}{2}B(\mathbf{u}, \mathbf{u}) - F_1(\mathbf{u})\right) \quad \forall \mathbf{u} \mid \mathbf{N}\cdot\mathbf{u} - g \leq 0 \quad \text{on } \Gamma_c. \tag{10}$$

Using the finite element discretization, the equivalent minimization problem given by (10) becomes

$$\min \{\tfrac{1}{2}\mathbf{u}^T\mathbf{K}\mathbf{u} - \mathbf{F}_1^T\mathbf{u}\} \quad \forall \mathbf{u} \mid \mathbf{A}\mathbf{u} \leq \mathbf{g}. \tag{11}$$

where $\mathbf{F}_1$ is the assembled force vector obtained by the discretization of the term f_1 given by equation (9). The constraints $\mathbf{A}\mathbf{u} \leq \mathbf{g}$ represent the assembly of the kinematic contact conditions at the candidate contact nodes on the candidate contact surface Γ_c. Here, $\mathbf{K}$ represents the total stiffness matrix resulting from the discretization of term $B(\cdot, \cdot)$. The minimization problem given in (11) representing the equivalent QP problem is solved using the projected gradients search method, which is described in details in Gill et al.[16]

The solution of step I provides an estimate of the displacement field from which the extent of the actual contact surface, which is readily provided by the active set of constraints, together with the normal tractions on it, are calculated. These data will be necessary to start the solution of the second step detailed in the following sub-section.

3.2 Special Case II: prescribed normal stress on a known contact surface Γ_c

Here, the actual contact surface, denoted also as Γ_c, is assumed to be known together with the normal stresses σ_N on it. Therefore, VI(3) reduces to

$$B(\mathbf{u}, \mathbf{v}-\mathbf{u}) + j(\mathbf{v}) - j(\mathbf{u}) \geq f_2(\mathbf{v}-\mathbf{u}) \quad \forall \mathbf{v}, \tag{12}$$

where $a(\cdot, \cdot)$ is as defined in (3) and,

$$j(\mathbf{v}) = \int_{\Gamma_c} \mu \, |\sigma_N| \, |v_T| \, ds, \tag{13}$$

and

$$f_2(\mathbf{v}) = f(\mathbf{v}) + \int_{\Gamma_c} \sigma_N v_N \, ds. \tag{14}$$

with $f(\cdot)$ is as defined in (3).

It has been shown by Glowinski et al.[15] that the solution of VI(12) is obtained by minimizing of an equivalent energy functional π given by

$$\pi(\mathbf{u}) = \tfrac{1}{2}B(\mathbf{u}, \mathbf{u}) - f_2(\mathbf{u}) + j(\mathbf{u}), \tag{15}$$

subject to a set of *equality* constraints resulting from the knowledge of the actual contact surface Γ_c. The main difficulty here is that the functional $\pi(\mathbf{u})$ is non-differentiable. In order to overcome this difficulty, the technique of regularization was used by Kikuchi and Oden.[9] This technique was further enhanced by Refaat and Meguid[12] to *explicitly* impose the contact constraints through the use of Lagrange multipliers. this non-differentiable minimization problem was also solved by Refaat and Meguid[13] through a sequence of quadratic programming sub-problems and applied to the case of elastic contact with small deformations.

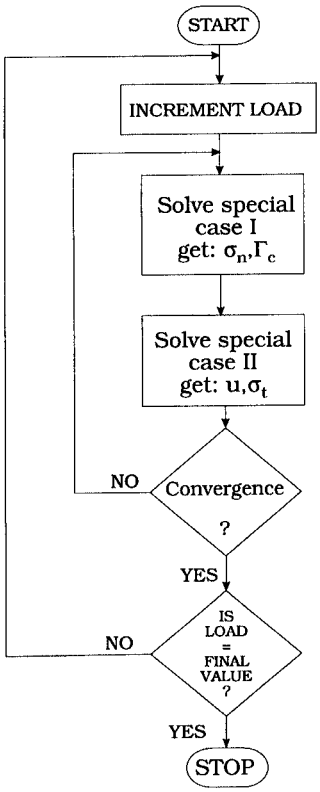


Fig. 4. A two-step algorithm for the solution of the general variational inequality.

https://doi.org/10.1017/S026357479800054X Published online by Cambridge University Press

In this work, we will develop a new successive approximation solution based on the elimination of the qauality constrains and regularization. This new method will reduce the size of the problem and enhance the speed of convergence.

It is now appropriate to use the finite element to discretize the domain of the finger and that of the manipulated body. In addition, we will describe the tangential components of the relative sliding displacement at contact nodes in terms of the nodes displacement as follows: for a node i on the contact surface Γ_c of the finger, the tangential component of the relative sliding displacement between the finger and the manipulated body will be denoted as v_i. In the case of plane problems, v_i can be expressed as

$$v_i = (u_x^i - u_x^j)\cos\theta + (u_y^i - u_y^j)\sin\theta \tag{16}$$

where the different terms are provided in Figure 5. The above expression is applied to each contact node on the contact surface of the finger, resulting in m equations that can be assembled in a matrix form; as follows:

$$\mathbf{v} = \mathbf{T}\mathbf{u}. \tag{17}$$

Therefore, the discrete form of the functional $j(\cdot)$ can be written as

$$j(\mathbf{v}) = \sum_{i=1}^{m} Fs_i\,|v_i| \tag{18}$$

with Fs_i being defined as $\mu\,|\sigma_{Ni}|\,A_i$. Substitution in the expression of the functional $\pi(\mathbf{u})$ lead to the current equivalent minimization problem

$$\begin{aligned} &\min\ \pi(\mathbf{u}) = \tfrac{1}{2}\mathbf{u}^T\mathbf{K}\mathbf{u} - \mathbf{F}_2^T\mathbf{u} + \sum_{i=1}^{m} \mathbf{F}\mathbf{s}_i\,|T_i\cdot\mathbf{u}| \\ &\text{subj.}\quad \mathbf{A}_o u = \mathbf{g}_o. \end{aligned} \tag{19}$$

with T_i is the ith row of the matrix $\mathbf{T}$ and $\mathbf{A}_o u = \mathbf{g}_o$ represent the the assembly of the prescribed displacements together with the active constraint set identified in step I of the two step algorithm; resulting in a total of $m + n_0$ constraints.

Because all the constraints are linear, we will be able to elimiante an equal number of variables from the functional $\pi(\mathbf{u})$ and reduce the problem to an

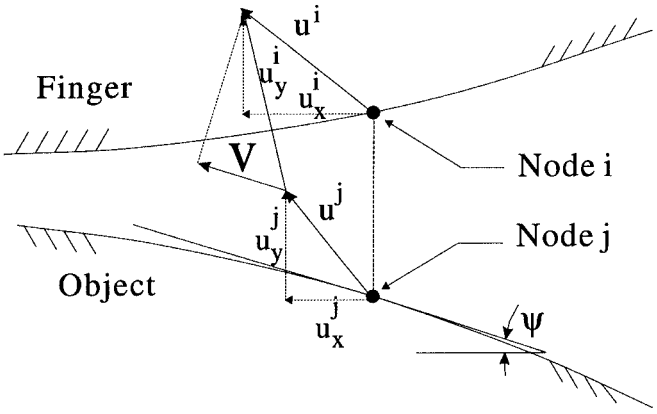


Fig. 5. Modelling of the tangential displacements in plane problems.

unconstrained minimization problem. This is accomplished by writing the constraints set in the form

$$\mathbf{u}_c = \mathbf{A}\mathbf{u}_f - \mathbf{g} \tag{20}$$

with the vector $\mathbf{u}_c$ of the variables to be eliminated is of dimension $m + n_o$ and that of $\mathbf{u}_f$ representing the remaining degrees of freedom of dimension $n - (m + n_o)$, where n is the total degrees of freedom. We then partition the matrices $\mathbf{K}, \mathbf{F}_2$ and $\mathbf{T}$ according to the corresponding elements of the vectors $\mathbf{u}_c$ and $\mathbf{u}_f$ into the following form

$$\mathbf{K} = \begin{bmatrix} \mathbf{K}_c & \mathbf{K}_{cf} \\ \mathbf{K}_{cf}^T & \mathbf{K}_f \end{bmatrix}, \tag{21}$$

$$\mathbf{F}_2 = \begin{bmatrix} \mathbf{R}_c \\ \mathbf{R}_f \end{bmatrix}, \tag{22}$$

and

$$\mathbf{T} = [\mathbf{T}_c \quad \mathbf{T}_f]. \tag{23}$$

By substitution into (19) and elimiating the vector $\mathbf{u}_c$ using (20), we obtain the reduced form of functional $\pi(\cdot)$, as follows:

$$\pi(\mathbf{u}_f) = \tfrac{1}{2}\mathbf{u}_f^T\mathbf{K}_e\mathbf{u}_f - \mathbf{R}_e^T\mathbf{u}_f + \sum_{i=1}^{m} \mathbf{F}\mathbf{s}_i\,|\mathbf{T}_{ei}\mathbf{u}_f + \alpha_i|, \tag{24}$$

where,

$$\mathbf{K}_e = \mathbf{K}_f + \mathbf{A}^T\mathbf{K}_c\mathbf{A} + 2\mathbf{A}^T\mathbf{K}_{cf}, \tag{25}$$

$$\mathbf{R}_e = \mathbf{R}_f + \mathbf{A}^T\mathbf{R}_c + \tfrac{1}{2}(2\mathbf{K}_{cf}^T + \mathbf{A}^T + \mathbf{A}^T\mathbf{K}_c)\mathbf{g}, \tag{26}$$

$$\mathbf{T}_e = \mathbf{T}_c\mathbf{A} + \mathbf{T}_f, \tag{27}$$

and

$$\alpha = -\mathbf{T}_c\mathbf{g}. \tag{28}$$

Now, in order to solve the current unconstrained non-differentiable minimization problem, we will adopt the technique of regularization. We will regularize the absolute value function $|\cdot|$ using the following expression

$$|v| \to \phi_\epsilon(v) = \begin{cases} v - \dfrac{\epsilon}{2} & v > \epsilon \\ \dfrac{1}{2\epsilon}v^2 & |v| \le \epsilon \\ \dfrac{\epsilon}{2} - v & v < -\epsilon. \end{cases} \tag{29}$$

Writing $v_i = \mathbf{T}_{ei}\mathbf{u}_f + \alpha_i$, $i = 1, \ldots, m$, then the regularized form of the functional $\pi(\mathbf{u}_f)$ is now given by

$$\pi_\epsilon(\mathbf{u}_f) = \tfrac{1}{2}\mathbf{u}_f^T\mathbf{K}_e\mathbf{u}_f - \mathbf{R}_e^T\mathbf{u}_f + \sum_{i=1}^{m} \mathbf{F}\mathbf{s}_i\phi_\epsilon(v_i). \tag{30}$$

which attains its minimum when $\partial\pi_\epsilon/\partial\mathbf{u}_f = \mathbf{0}$, or when

$$\mathbf{K}_e\mathbf{u}_f - \mathbf{R}_f + \sum_{i=1}^{m} \mathbf{F}\mathbf{s}_i\mathbf{T}_{ei}^T\frac{d\phi_\epsilon(v_i)}{dv_i} = \mathbf{0}, \tag{31}$$

https://doi.org/10.1017/S026357479800054X Published online by Cambridge University Press

with

$$\frac{\phi'_\epsilon(v_i)}{dv_i} = \begin{cases} 1 & \mathbf{T}_{ei}\mathbf{u}_f + \alpha_i > \epsilon \\ \dfrac{\mathbf{T}_{ei}\mathbf{u}_f + \alpha_i}{\epsilon} & |\mathbf{T}_{ei}\mathbf{u}_f + \alpha_i| \le \epsilon \\ -1 & \mathbf{T}_{ei}\mathbf{u}_f + \alpha_i < -\epsilon. \end{cases} \quad (32)$$

Therefore, the $(j+1)^{\text{th}}$ iteration of the successive approximation solution of the set of nonlinear equations provided by (31) is now given according to

$$\mathbf{u}_f^{(j+1)} = \mathbf{K}_e^{-1}\left(\mathbf{R}_f + \sum_{i=1}^{m} \mathbf{Fs}_i \mathbf{T}_{ei}^T \phi'_\epsilon(\mathbf{T}_{ei}\mathbf{u}_f + \alpha_i)\right)^{(j)}. \quad (33)$$

The above scheme begins with $j = 0$ and $\mathbf{u}_f$ is the respective partition obtained from the solution provided by step I of the two step algorithm.

It is worth noting here that in the case of $m = 0$, i.e. no contact, the iterative scheme given by (33) will restore the original FE solution with reduced rigid body degrees of freedom. Therefore equation (33) represents a consistent solution scheme.

4 CASE STUDY

The main purpose of this study is to determine the compliance of a gripper in contact with a generic object using variational inequalities.

In view of the symmetry of the multi-fingered gripper considered, the model is idealized using one finger and the simple generic object shown in Figure 6. The object and the finger were discretized using four-noded quadrilateral elements with a high density mesh at the candidate contact surface.

In order to calculate the compliance of the gripper-object considered, the right hand side of the gripper is constrained in the horizontal direction and is allowed to slide in the vertical direction where the force is applied. The computed compliance is normalized by point-contact compliance C_o and the applied force is normalized by the critical yielding force F_{cr}.

Let us first consider the case of a relatively rigid object in comparison with the finger. the compliance of the system is thus calculated using the new method and the results are depicted in Figure 7 for different coefficients of friction. These results are for a concave contact surface with a radius of curvature of 21 mm. Surprisingly, the results of Figure 7 reveal that the compliance computed by the new method differ by as much as 15% of that corresponding to the point contact assumption. The figure also reveals that the friction at the interface has a marked effect on the value of the compliance at low level of forces. Specifically, at very small F/F_{cr}, a sudden drop in the value of the compliance at low level of forces. Specifically, at very small F/F_{cr}, a sudden drop in the value of the compliance is observed. This is attributed to the slip-stick regions present at these low levels of forces.

The newly developed algorithm also allows us to describe the stress distribution inside the finger. Figure 8 shows the contour of the equivalent (von Mises) stresses corresponding to an externally applied force of 40% of the yielding force. The figure shows the rapid increase in the equivalent stress level at and near the contact region. These values should be considered carefully in the design of the gripper.

Let us now examine the effect of elasticity of the manipulated object on the effective compliance of the system. This was conducted by varying the elastic moduli ratio of the object and the finger. The results which are shown in Figure 9 depict the dependence of the compliance upon that ratio. Typically, the figure indicates that the compliance can vary by as much as 8% for a moduli ratio of unity. The extent of these changes will ultimately depend upon the relative size and geometry of the gripping finger and that of the object.

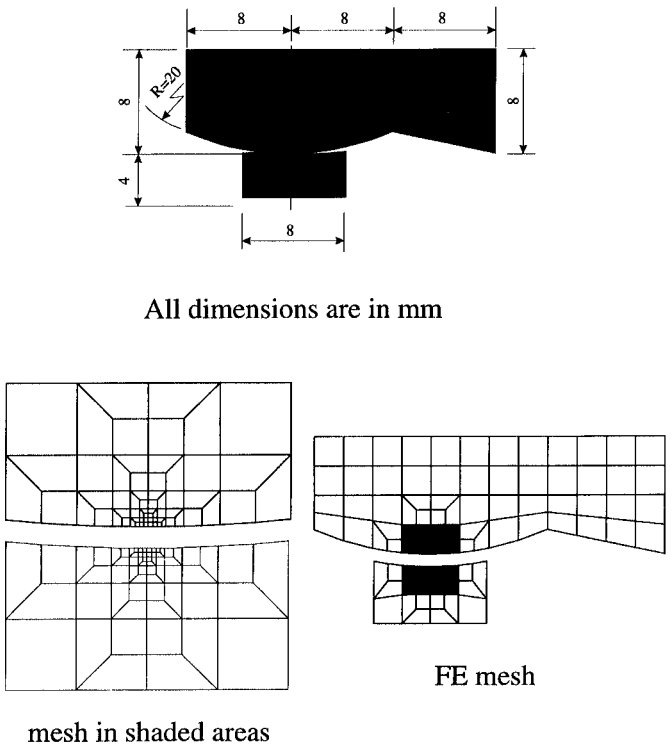


Fig. 6. Geometry and FE meshes for a compliant finger and a generic object.

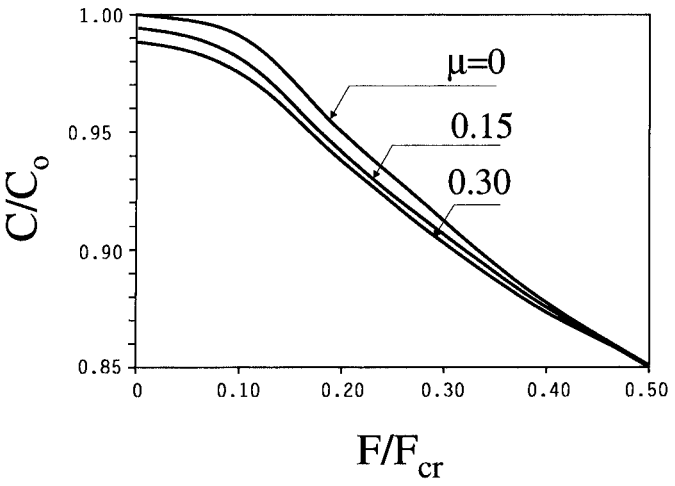


Fig. 7. Effect of the coefficient of friction on the variation of the compliance with the applied force.

https://doi.org/10.1017/S026357479800054X Published online by Cambridge University Press

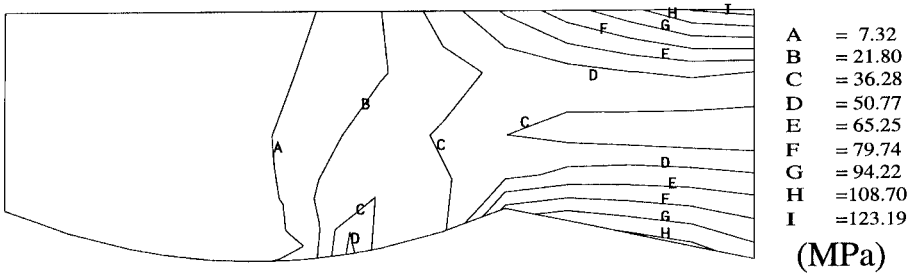


Fig. 8. Von Mises stress contours in the gripping finger for a force of $0.4F_{cr}$.

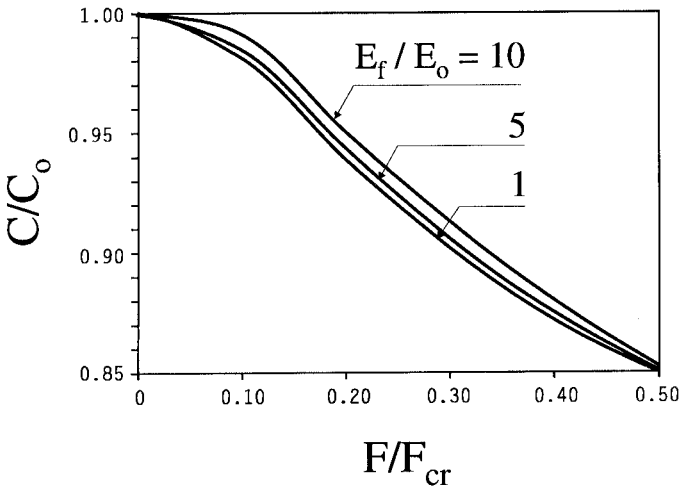


Fig. 9. Effect of the object elasticity on the variation of the gripper compliance.

5 CONCLUSIONS

In this study, we adopt Quadratic Programming and regularization techniques, in a two-step algorithm, to treat the contact problem arising in compliant robotic grippers. By avoiding the use of user defined parameters currently adopted in most contact element formulations, the contact problem was treated effectively and efficiently. The current formulation would guarantee the imposition of the active kinematic contact constraints account for the effect of friction through the use of an appropriate regularization technique in the virtual work expressions. The method is applied to the analysis of a detailed case study for the calculation of the gripper compliance and showed the effect of the local distribution of the contact forces on the total compliance of the gripper. It has been shown that the actual value of the compliance can vary by as much as 15% from that based on the point-contact assumption. It is hoped that this work will be a useful tool in the design of efficient controllers for robotic system involving compliant grippers.

ACKNOWLEDGEMENTS

This work was supported in part by the Institue of Robotics and Intelligent Systems (IRIS) and in part by the Natural Sciences, Enginering Research Council of Canada (NSERC) and ALCOA Foundation of the USA.

References

1. M.R. Cutkosky, *Robotic Grasping and Fine Manipulation* (Kluwer Academic Publishers Group, The Netherlands, 1985).
2. M.R. Cutkosky, "On Grasp Choice, Grasp Models, and the Design of Hands for Manufacturing Tasks" *IEEE Transactions on Robotics and Automation* **5,** No. 3, 151–165 (1989).
3. M.R. Cutkosky and I. Kao, "Computing and Controlling the Compliance of a Robotic Hand" *IEEE Transactions on Robotics and Automation* **5,** No. 2,269–274 (1989).
4. E.E. Rosheim, *Robot Wrist Actuators* (John Wiley and Sons Inc., New York, 1989).
5. S.T. Venkataraman and T. Iberall, *Dextrous Robot Hands* (Springer Verlag New York Inc., New York, 1990).
6. T. Speeter, "Three-dimenaional Finite Element Analysis of Elastic continua of Tactile Sensing" *Int. J. Robotics Research* **11,** No. 1, 1–19 (1992).
7. K.L. Johnson, *Contact Mechanics* (Cambridge University Press, Cambridge, 1985).
8. G.M.L. Gladwell, *Contact Problems in the Classical Theory of Elasticity* (Alphen aan den Rijn: Sijthoff and Noordhoff, The Netherlands, 1980).
9. N. Kikuchi and J.T. Oden, *Contact Problems in Elasticity: A Study of Variational Inequalities and Finite Element Methods* (SIAM, Elsevier Science Publishers, 1988).
10. J.B. Böhm, "A Comparison of Different Contact Algorithms with Applications" *Computers and Structures* **26,** 207–221 (1987).
11. G.E. Starvroulakis, P.D. Panagiotopoulos and A.M. Al-Fahd, "On the Rigid Body Displacements and Rotations in Unilateral Contact Problems and Applications" *Computers and Structures* **40,** 599–614 (1991).
12. M.H. Refaat and S.A. Meguid, "On the Elastic Solution of Frictional Contact Problems Using Variational Inequalities" *Int. J. Mechanical Sciences* **36,** No. 4, 329–342 (1994).
13. M.H. Refaat and S.A. Meguid, "A Novel Finite Element Approach to Frictional Contact Problems" *Int. J. Numerical Methods in Engineering* **39,** 3889–3902 (1996).
14. S.A. Meguid, P. Papanikos and M.H. Refaat, "Finite Element Analysis of Dovetail Joints in Aeroengine Discs Using Interface Elements" *Proceedings of the International Conference on Computational Methods in Engineering,* Singapore (1992) pp. 1373–1378 (1992).
15. R. Glowinski, T.C. Lions and R. Tremolieres, *Numerical Analysis of Variational Inequalities* (North Holland Publishing Company, Amsterdam, 1981).
16. P.E. Gill, W. Murray and M.H. Wright, *Practical Optimization* (Academic Press, London 1981).

https://doi.org/10.1017/S026357479800054X Published online by Cambridge University Press

NOTATION

A_i: Contact area at node i

F: Discretized nodal load vector

K: Assembled stiffness matrix

N: Normal vector $\{N_1 \ N_2 \ N_3\}^T$,

$$N_1 = \frac{\partial \psi}{\partial x} \Big/ \sqrt{1 + \left(\frac{\partial \psi}{\partial x}\right)^2 + \left(\frac{\partial \psi}{\partial y}\right)^2},$$

$$N_2 = \frac{\partial \psi}{\partial y} \Big/ \sqrt{1 + \left(\frac{\partial \psi}{\partial x}\right)^2 + \left(\frac{\partial \psi}{\partial y}\right)^2}$$

and

$$N_3 = -1 \Big/ \sqrt{1 + \left(\frac{\partial \psi}{\partial x}\right)^2 + \left(\frac{\partial \psi}{\partial y}\right)^2}$$

g: Normalized gap

g: Vector of assembly of normalized gaps over the candidate contact surface

s: Surface area

t: Surface tractions on boundary Γ_t

f_i: Body force in domain the Ω of the compliant finger

v: A displacement vector

w: A virtual displacement vector

x, y, z: Cartesian coordinate system

μ: Coefficient of friction

σ_{ij}: Stress tensor

ϵ_{ij}: Strain tensor

σ_n, σ_t: Normal and tangential contact stresses

ϕ, ψ: Functions representing candidate contact surfaces; see Figure 3 for details

Γ_c: Candidate or actual contact surface

Γ_d: Boundary with a prescribed displacement field

Subscripts t and n denote tangential and normal components, respectively.

Superscript T denotes transpose of a matrix.

https://doi.org/10.1017/S026357479800054X Published online by Cambridge University Press